Development of an Organic Plastic Scintillator-based Muon Veto Operating at Sub-Kelvin Temperatures for the NUCLEUS Experiment

A. Erhart[1,2] · V. Wagner[1] · L. Klinkenberg[1] · T. Lasserre[2] · D. Lhuillier[2] ·
C. Nones[2] · R. Rogly[2] · V. Savu[2] · R. Strauss[1] · M. Vivier[2] · on behalf of the
NUCLEUS collaboration

Abstract

The NUCLEUS experiment aims at measuring the coherent elastic scattering of nuclear reactor antineutrinos off nuclei using cryogenic calorimeters. Operating at an overburden of 3 m.w.e., muon-induced backgrounds are expected to be dominant. It is therefore essential to develop an efficient muon veto, with a detection efficiency of more than 99 %. This will be realized in NUCLEUS through a compact cube assembly of plastic scintillator panels. In order to prevent a large unshielded area where the cryostat intersects the shielding arrangement without unnecessarily increasing the induced detector dead time, a novel concept has been investigated, featuring a plastic scintillator-based active muon veto operating inside the NUCLEUS cryostat at sub-Kelvin temperatures. The verification of the key physical aspects of this cryogenic muon veto detector led to the first reported measurements of organic plastic scintillators at sub-Kelvin temperatures. The functionality of the principal scintillation process of organic plastic scintillators at these temperatures has been confirmed. On the basis of these findings, a disk-shape plastic scintillator equipped with wavelength shifting fibers and a silicon photomultiplier to guide and detect the scintillation light has been developed. The NUCLEUS cryogenic muon veto will be the first of its kind to be operated at sub-Kelvin temperatures.

Keywords Plastic scintillator · SiPM · WLS fibers · Muon veto

✉ A. Erhart
andreas.erhart@tum.de

1   Physik-Department, Technische Universität München, 85748 Garching, Germany

2   IRFU, CEA, Université Paris Saclay, 91191 Gif-sur-Yvette, France

1 Introduction

The occurrence of neutral-current interactions within the Standard Model of Particle Physics implies the coupling of neutrinos to quarks through exchange of a neutral Z boson [1]. In 1974, Daniel Z. Freedman concluded the existence of elastic neutrino-nucleus scattering—a process which is not limited by an energy threshold and thus predicts strong coherent effects at very low neutrino energies of $\mathcal{O}(10$ MeV) [2]. The exploration of coherent elastic neutrino-nucleus scattering (CEνNS) opens a new window to study the fundamental properties of neutrinos and allows to probe various scenarios of physics beyond the Standard Model (see [3–5] and references therein).

The NUCLEUS experiment aims to employ gram-scale fiducial-volume cryogenic calorimeters with a demonstrated ultra-low threshold of $E_{th} = 19.7$ eV for nuclear recoils [6]. The new experimental site designated for the installation of the NUCLEUS experiment is a 24 m^2 basement room in an administrative building situated in between the two 4.25 GW$_{th}$ reactor cores of the Chooz nuclear power plant (located in the Ardennes department in northeastern France). The site features an expected antineutrino flux as high as $2.1 \cdot 10^{12}$ $\bar{\nu}_e$/(s·cm^2) with an average antineutrino energy as low as 1.5 MeV [7]. Besides the high rate and low energy that make nuclear reactors favorable neutrino sources for an accurate measurement of the CEνNS cross section, a low residual background rate in the target detectors is mandatory. Operating at an overburden of only 3 m.w.e., muon-induced events are expected to be the dominant source of background [8]. The muon-induced neutrons, which are particularly harmful due to the same experimental signature as the sought-for CEνNS (i.e., a nuclear recoil) can be reduced passively via moderation and absorption in polyethylene. Additionally, for an active background suppression of prompt muon-associated events and to reach the benchmark background index of 100 counts / (keV kg day) in the sub-keV region [7], a muon veto with a detection efficiency of more than 99 % is required. For the NUCLEUS experiment, the muon veto (shown schematically in Fig. 1) will consist of a compact cube assembly of 28 single organic plastic scintillator panels equipped with wavelength shifting fibers and silicon photo multipliers (SiPM) to collect and detect the scintillation light. Each panel will be enclosed in a light-tight aluminium box and placed around the NUCLEUS target detector covering the largest possible part of its 4 π steradians of solid angle. The expected muon identification rate for the full assembly of $\sim$ 325 Hz implies an induced target detector dead time of only 1.6 %, assuming a 50 μs veto time window centered on the arrival time of each identified muon. Inevitably, a large unshielded area remains in the upper side of the experiment, where the cryostat containing the NUCLEUS detector and its support structure will be inserted (see Fig. 1). In order to close this gap without unnecessarily increasing the induced target detector dead time, a novel concept has been developed [9], consisting of a plastic scintillator-based disk-shape active muon veto operating inside the NUCLEUS cryostat at sub-Kelvin temperatures.
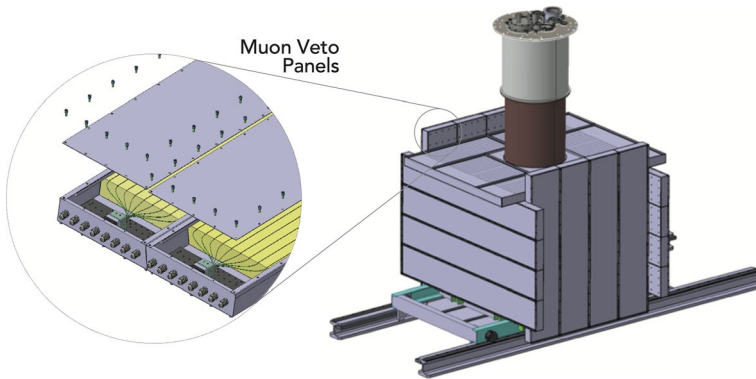
Fig. 1 Schematic drawing of the NUCLEUS experimental setup. The NUCLEUS cryostat containing the target detectors is shielded by several layers of active and passive materials. The outermost layer is an active muon veto, consisting of 28 single organic plastic scintillator panels each enclosed in a light-tight aluminium box and placed hermetically around the NUCLEUS cryostat. The single muon veto panels (*Left Zoom-In*) are equipped with wavelength shifting fibers and SiPMs to collect and detect the scintillation light.

2 Detector Concept and Integration with the Cryogenic Infrastructure

The NUCLEUS cryogenic muon veto will be installed inside a commercial LD 400 ^{3}He / ^{4}He dry dilution refrigerator provided by Bluefors [10]. The detector concept (shown schematically in Fig. 2) consists—analogously to the NUCLEUS external muon veto concept—of plastic scintillator instrumented with a fiber-based light-guide system together with a SiPM-based read-out system. It is foreseen to install a disk of the polystyrene-based plastic scintillator UPS 923-A [11] with an outer diameter of 297 mm, a height of 50 mm and a total mass of ∼ 3.6 kg underneath the mixing chamber plate of the NUCLEUS cryostat. The disk features nine bended grooves, each of which guides a BCF-91A wavelength shifting fiber [12] through the interior of the plastic scintillator. The fibers are glued via the two component clear epoxy resin BC-600 [13] into the grooves, assuring thorough fixation and maximization of the contact surface. An inner hole with a diameter of 45 mm is required for the feed-through of the detector support structure. The scintillation light is collected by the fibers and guided through the cryostat vessels toward a gain-stabilized and pre-amplified KETEK PE3325-WB TIA TP SiPM module [14], which is mounted on the bottom of the 300 K plate inside the cryostat and thus operating at constant room temperature. Together, the cryogenic muon veto and the passive shielding (consisting of lead and polyethylene) constitute the inner shielding of the NUCLEUS experiment. The mechanical holding structure of the inner shielding has been conceived such that a copper disk, connected via three Kevlar tie rods to the central tube of the cryostat, serves both as mechanical support structure and thermal bath for the plastic scintillator disk of the cryogenic muon veto. It is thermally coupled to the still stage of the cryostat and thus thermalized at ∼ 850 mK.
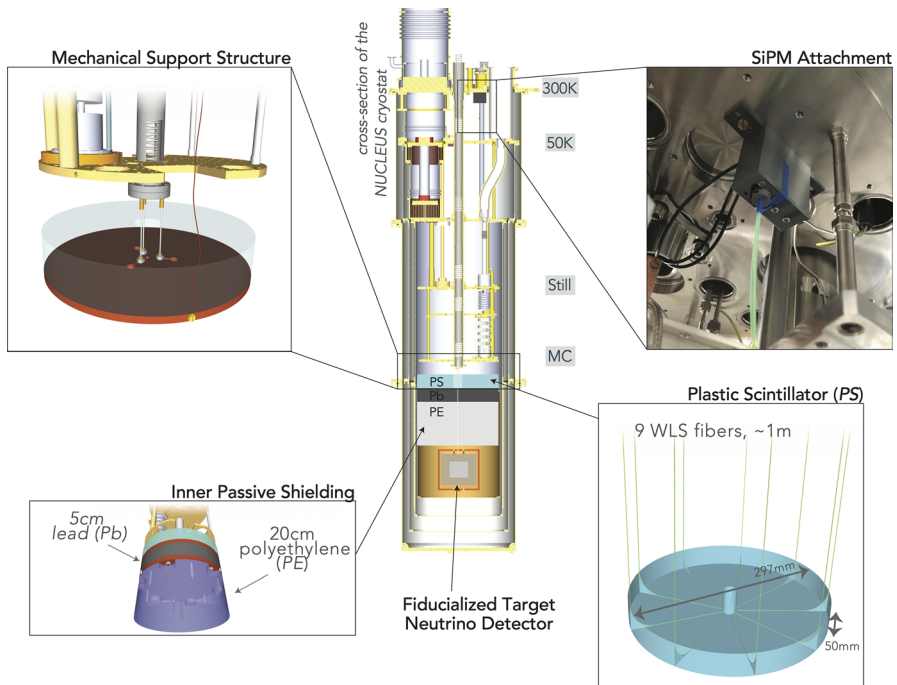
Fig. 2 Schematic drawing of the NUCLEUS cryogenic muon veto detector concept, with a cross section of the NUCLEUS cryostat (*Center*) and zoom-in on the plastic scintillator disk (*Bottom Right*), the SiPM attachment to the 300 K plate (*Top Right*), the inner passive shielding (*Bottom Left*) and the mechanical support structure (*Top Left*).

3 Low Temperature Behavior of Organic Plastic Scintillators

Given the scarcity of experimental studies on the thermalization behavior and the scintillation mechanism of organic plastic scintillators at sub-Kelvin temperatures, a proof-of-concept detector has been conceived in order to validate the feasibility of the intended NUCLEUS cryogenic muon veto detector concept. To this end, smaller-scale cylindrical pieces of plastic scintillators with a height and a diameter of 42 mm each and four of the BCF-91A wavelength shifting fibers glued into small grooves on the side were assembled, mimicking the envisaged final design. This cryogenic muon veto prototype is being operated within a customized copper holder on top of the still stage of the NUCLEUS cryostat and thermally coupled to a temperature of $T_{still} \sim 850$ mK. The temperature of the plastic scintillator can be monitored with a calibrated resistance thermometer on its top surface, and the light from the scintillator is guided through the fibers to a SiPM mounted at the bottom of the 300 K plate of the cryostat. One additional external scintillator panel coupled to a PMT is positioned underneath the cryogenic muon veto prototype outside the cryostat and is used to select muon events by means of a twofold coincidence in the PMT and the SiPM.

3.1 Thermalization Behavior of Organic Plastic Scintillators

The thermalization behavior of organic plastic scintillators has been investigated for a sample of the polyvinyltoluene-based plastic scintillator EJ-204 [15]. The temperature curves of the still stage T_{still} (*Blue*) and of the upper side of the cylindrical plastic scintillator T_{PS} (*Red*) are shown in Fig. 3. Starting from 100 K, the still stage reaches its base temperature $T_{still} \approx 0.86$ K after ~ 27 h. The plastic scintillator sample fully thermalizes within ~ 52 h (with the time onset defined as the point in time in which $T_{still} = 100$ K), corresponding to a delay in thermalization time of the plastic scintillator w.r.t. the still stage of ~ 25 h. The cooling performance of the dry dilution refrigerator has not noticeably degraded due to the installation of the plastic scintillator piece.

In summary, this observation states that the cooling of the NUCLEUS cryogenic muon veto to its operating temperature is achievable on a time scale completely reconcilable with the operational parameters envisaged for the NUCLEUS cryogenic infrastructure and is thus not expected to considerably affect them.

3.2 Temperature Dependence of the Muon Pulse Shape

The temperature dependence of the pulse shape of a muon crossing through organic plastic scintillators has been studied for a sample of the polystyrene-based plastic scintillator UPS 923-A. This resulted, to the best of the authors' knowledge, in the first reported measurements of organic plastic scintillators at sub-Kelvin temperatures, confirming the functionality of their principal scintillation process down to these temperatures. Two examples of muon pulses with comparable amplitudes, captured at room temperature $T_{room} \approx 293$ K and at still temperature $T_{still} \approx 850$ mK, are shown in Fig. 4. The pulse decay time of the scintillator, which is defined as the
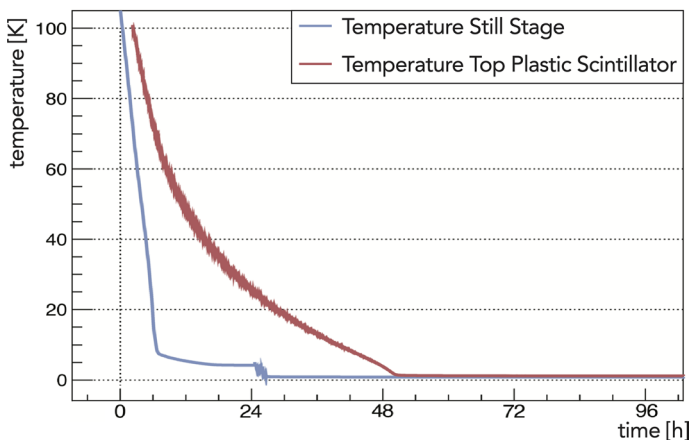
Fig. 3 Temperature curves of the upper side of the plastic scintillator prototype (*Red*) and of the still stage (*Blue*) during cool-down of the cryostat. The time onset is defined when the still stage reaches a temperature of $T_{still} = 100$ K. The still stage reaches its base temperature of $T_{still} \approx 0.86$ K within 27 h. The thermal equilibrium temperature of the plastic scintillator $T_{PS} \approx 1.19$ K is reached within 52 h.
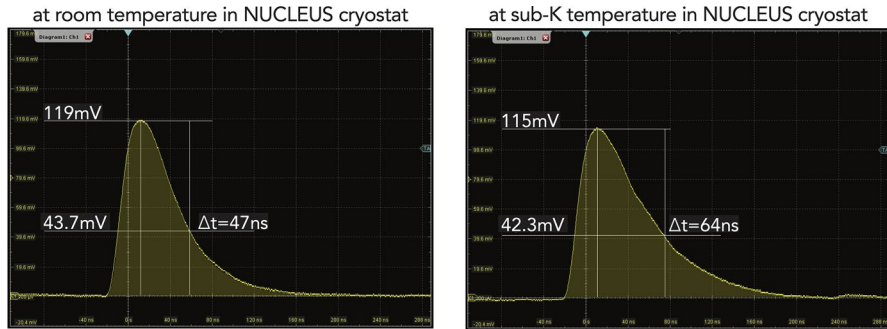
Fig. 4 Exemplary muon pulses recorded at room temperature $T_{room} \approx 293$ K (*Left*) and at still temperature $T_{still} \approx 850$ mK (*Right*). The pulses peak at values of 119 mV and 115 mV, respectively. The pulse decay time of the muon pulse increases from $t_{decay,\,room} = 47$ ns at room temperature to $t_{decay,\,still} = 64$ ns at still temperature. Averaged for a number of pulses, it can be observed that the pulse decay time is enhanced by 32 % at sub-Kelvin temperature.

time after which the pulse has returned to $1/e$ of its peak value, has been observed to increase from $t_{decay,\,room} = 47$ ns at room temperature to $t_{decay,\,still} = 64$ ns at still temperature. On average, the pulse decay time has been found to increase by ~ 32 % toward lower temperatures. The timing of the muon coincidences will be governed by the slow rise time of $\mathcal{O}(100~\mu s)$ of the cryogenic target neutrino detectors. Hence, the enhancement of the muon pulse decay time of $\mathcal{O}(10$ ns$)$ observed in the cold plastic scintillator is negligibly small compared to the 50 μs veto time window and does not impact the practical operation of the NUCLEUS muon veto.

In the course of the featured measurements, the main components of the NUCLEUS cryogenic muon veto detector—namely the SiPM mounting in the inside of the cryostat, the associated fiber guidance and the plastic scintillator to be thermalized—have been installed and operated successfully. The practical operation of a muon veto based on an organic plastic scintillator inside a running dry dilution refrigerator has thus been demonstrated.

4 Detector Commissioning at Room Temperature

On the basis of these findings, the disk-shape plastic scintillator-based muon veto has been assembled and commissioned at room temperature. Figure 5 shows the full charge spectrum recorded with the plastic scintillator disk (*Gray*), which features a pedestal, a region for low energetic background events (i.e., ambient gammas from natural radioactivity) and muon events following a Landau-like distribution. By operating the disk-shape scintillator in a threefold coincidence with two external scintillator panels sandwiching it from top and from bottom, the charge spectrum can be restricted to exclusively muon events (*Red*). However, the coincidence criterion constrains the angular acceptance of impinging muons and hence their total rate. The conceived muon veto design allows unambiguous identification of the
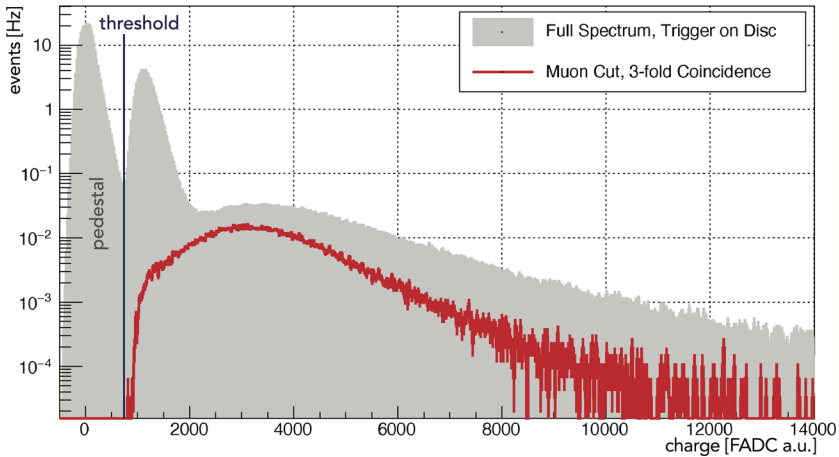
Fig. 5 Full charge spectrum recorded with the plastic scintillator disk (*Gray*) and restriction to exclusively muon events via coincidence criterion (*Red*). The integrated charge of the pulse is an estimate for the energy deposited by a particle event. The full spectrum features a pedestal, a region for low energetic background events cut at a certain threshold and muon events following a Landau-like distribution. The most probable value of the muon distribution can be determined with a local Gaussian fit to be ~ 3063 *FADC a.u.*, corresponding to muons impinging vertically with an average energy deposition in the plastic scintillator of around 10 MeV. The restriction of the angular acceptance of muons leads to a decrease of their rate.

muon events and features sufficient discrimination capability between muons and ambient gammas.

5 Conclusion and Outlook

By investigating the thermalization behavior of organic plastic scintillators and the temperature dependence of the muon pulse shape, the foundations for the development of an organic plastic scintillator-based muon veto operating at sub-Kelvin temperatures inside the NUCLEUS cryostat have been laid. Within the framework of the work presented, the intended detector concept—i.e., a plastic scintillator-based detector equipped with a fiber-based light-guide system together with a SiPM-based read-out system—has been proven for its applicability inside a running dry dilution refrigerator and commissioned at room temperature. A detailed characterization of the disk on its efficiency, its capability to separate muons and gammas, and its light yield homogeneity is ongoing. Furthermore, the phenomenology of organic plastic scintillators at different temperatures, in particular possible temperature dependencies of the detectors' light output, is currently being investigated within the established experimental setup. For this purpose, the data acquisition has been recently upgraded with an FADC (Struck SIS3316) to record the pulse traces [16]. The first deployment of the cryogenic muon veto in coincidence with the external muon veto is planned for the commissioning of the NUCLEUS experiment, which will be carried out at Technical University of Munich in 2022-23.

Declarations

Conflict of interests The authors declare that they have no known competing financial interests or personal relationships that could have influenced the work reported in this paper. The data that support the findings of this study are available from the corresponding author, A. Erhart, upon reasonable request. All listed authors consent to the publication of the work.

References

1. F.J. Hasert et al., Observation of neutrino-like interactions without muon or electron in the Gargamelle neutrino experiment. Nucl. Phys. B **73**(1), 1–22 (1974). https://doi.org/10.1016/0550-3213(74)90038-8
2. D.Z. Freedman, Coherent effects of a weak neutral current. Phys. Rev. D **9**(5), 1389 (1974). https://doi.org/10.1103/PhysRevD.9.1389
3. J. Barranco et al., Probing new physics with coherent neutrino scattering off nuclei. JHEP **2005**(12), 021 (2005). https://doi.org/10.1088/1126-6708/2005/12/021
4. M. Lindner et al., Coherent neutrino-nucleus scattering and new neutrino interactions. JHEP **2017**(03), 097 (2017). https://doi.org/10.1007/JHEP03(2017)097
5. J. Billard et al., Prospects for exploring new physics in coherent elastic neutrino-nucleus scattering. JCAP **2018**(11), 016 (2018). https://doi.org/10.1088/1475-7516/2018/11/016
6. R. Strauss et al., Gram-scale cryogenic calorimeters for rare-event searches. Phys. Rev. D **96**(2), 022009 (2017). https://doi.org/10.1103/PhysRevD.96.022009
7. G. Angloher et al., Exploring CEνNS with NUCLEUS at the Chooz nuclear power plant. Eur. Phys. J. C **79**(12), 1–16 (2019). https://doi.org/10.1140/epjc/s10052-019-7454-4
8. G. Heusser, Low-radioactivity background techniques. Annu. Rev. Nucl. Part. Sci. **45**(1), 543–590 (1995). https://doi.org/10.1146/annurev.ns.45.120195.002551
9. A. Erhart, Development of an organic plastic scintillator based muon veto operating at sub-kelvin temperatures for the NUCLEUS experiment. *Master's Thesis, Technical University of Munich*. (2021). available at: https://mediatum.ub.tum.de/node?id=1631300
10. *Bluefors. LD 400^{3}He / ^{4}He Dilution Refrigerator*. available at: https://bluefors.com (2021 (04.10.2021))
11. *Institute for Scintillation Materials of NAS. Plastic Scintillator UPS 923-A*. available at: http://isma.kharkov.ua/en (2021 (04.10.2021))
12. *Saint Gobain. Wavelength Shifting Fibers BCF-91A*. available at: https://www.crystals.saint-gobain.com/products/scintillating-fiber (2021 (04.10.2021))
13. *Saint Gobain. Optical Cement BC-600*. available at: https://www.impexron.de/show_catalogue_pdf/161503/1 (2021 (13.05.2022))
14. *KETEK. Silicon Photomultipliers PE3325-WB TIA TP*. available at: https://www.ketek.net (2021 (04.10.2021))
15. *Eljen Technology. Plastic Scintillator EJ-204*. available at: https:// eljentechnology.com/products/plastic-scintillators (2021 (04.10.2021))

16. A. Erhart, et al., Development of an organic plastic scintillation Muon Veto operating at sub-kelvin temperatures. *article in preparation*